The Entropic Penalty of Ordered Water Accounts for Weaker Binding of the Antibiotic Novobiocin to a Resistant Mutant of DNA Gyrase: A Thermodynamic and Crystallographic Study‡

Geoffrey A. Holdgate, Alan Tunnicliffe,§ Walter H. J. Ward, Simon A. Weston, Gina Rosenbrock, Peter T. Barth, Ian W. F. Taylor, Richard A. Pauptit, and David Timms*

ZENECA Pharmaceuticals, Mereside, Alderley Park, Macclesfield, Cheshire SK10 4TG, U.K.

Received February 7, 1997; Revised Manuscript Received May 23, 1997⊗

ABSTRACT: Novobiocin is an antibiotic which binds to a 24 kDa fragment from the B subunit of DNA gyrase. Naturally occurring resistance arises from mutation of Arg-136 which hydrogen bonds to the coumarin ring of novobiocin. We have applied calorimetry to characterize the binding of novobiocin to wild-type and R136H mutant 24 kDa fragments. Upon mutation, the K_d increases from 32 to 1200 nM at 300 K. The enthalpy of binding is more favorable for the mutant ($\Delta H°$ shifts from −12.1 to −17.5 kcal/mol), and the entropy of binding is much less favorable ($T\Delta S°$ changes from −1.8 to −9.4 kcal/mol). Both of these changes are in the direction opposite to that expected if the loss of the Arg residue reduces hydrogen bonding. The change in heat capacity at constant pressure upon binding (ΔC_p) shifts from −295 to −454 cal mol^{-1} K^{-1}. We also report the crystal structure, at 2.3 Å resolution, of a complex between the R136H 24 kDa fragment and novobiocin. Although the change in ΔC_p often would be interpreted as reflecting increased burial of hydrophobic surface on binding, this structure reveals a small decrease. Furthermore, an ordered water molecule is sequestered into the volume vacated by removal of the guanidinium group. There are large discrepancies when the measured thermodynamic parameters are compared to those estimated from the structural data using empirical relationships. These differences seem to arise from the effects of sequestering ordered water molecules upon complexation. The water-mediated hydrogen bonds linking novobiocin to the mutant protein make a favorable enthalpic contribution, whereas the immobilization of the water leads to an entropic cost and a reduction in the heat capacity of the system. Such a negative contribution to ΔC_p, $\Delta H°$, and $T\Delta S°$ appears to be a general property of water molecules that are sequestered when ligands bind to proteins.

DNA gyrase is a bacterial type II DNA topoisomerase (EC 5.99.1.3) which uses the free energy of ATP hydrolysis to catalyze the negative supercoiling of double-stranded circular DNA (Reece & Maxwell, 1991). This function is essential for DNA replication and transcription and is performed by other enzymes in eukaryotes so that gyrase is a suitable target for antibacterial agents. The enzyme from *Escherichia coli* consists of two subunits, A and B, with molecular masses of 97 and 90 kDa, respectively, in an A_2B_2 tetramer. The A protein is responsible for DNA cleavage and rejoining, whereas the B protein contains the ATP-binding site. Currently, there are two classes of antibiotics that target gyrase: the synthetic quinolones (*e.g.* nalidixic acid) and the coumarin natural products (*e.g.* novobiocin, clorobiocin, and coumermycin A_1). The quinolones are thought to act by interfering with the DNA breakage−rejoining step on the A subunit (Maxwell, 1992), whereas the coumarins act at the B subunit by inhibiting ATP hydrolysis (Maxwell, 1993). Both have limitations and side effects, and novel gyrase inhibitors are still sought.

The structure of an entire type II topoisomerase has yet to be reported, but a useful model which gives mechanistic insight can be constructed from the known structures of complementary fragments (Berger et al., 1996; Wigley, 1996). The gyrase B subunit contains a 43 kDa N-terminal domain which includes the site of ATP hydrolysis and a 47 kDa C-terminal domain which interacts with the A subunit and probably DNA (Figure 1). The crystal structure of this 43 kDa N-terminal fragment complexed with adenylyl β,γ-imidodiphosphate (ADPNP)[1] has been reported (Wigley et al., 1991). ADPNP induces dimerization of the 43 kDa fragment in solution (Ali et al., 1993, 1995), and this fragment crystallizes as a dimer containing one bound ADPNP molecule per monomer. The binding evironment of the adenine ring of the ADPNP (Figure 2) is relevant to the present study. In particular, the adenine N3 aza nitrogen accepts a hydrogen bond from the hydroxyl group of Tyr-5′ from the N-terminal arm of the other monomer. The main chain carbonyl group of this residue forms a hydrogen bond across the dimer interface with the guanidinium group of Arg-136.

Each 43 kDa domain consists of two subdomains: an N-terminal subdomain (residues 2−220, 24 kDa) and a

‡ Coordinates have been deposited in the Brookhaven Protein Data Bank (ID code 1aj6).

* Author for correspondence. Phone: 01625-514656. Fax: 01625-583074. E-mail: dave.timms@alderley.zeneca.com.

§ Present address: Institut für Molekular Biotechnologie, Beutenbergstrasse 11, D-07708 Jena, Germany.

⊗ Abstract published in *Advance ACS Abstracts,* July 1, 1997.

[1] Abbreviations: ADPNP, 5′-adenylyl β,γ-imidodiphosphate; ΔASA_{ap} and ΔASA_{pol}, changes in apolar and polar accessible surface areas upon binding, respectively; ΔC_p, change in heat capacity at constant pressure upon binding; IPTG, isopropyl β-D-thiogalactoside; MES, 2-(*N*-morpholino)ethanesulfonic acid; Tris, tris(hydroxymethyl)aminomethane.

S0006-2960(97)00294-8 CCC: $14.00

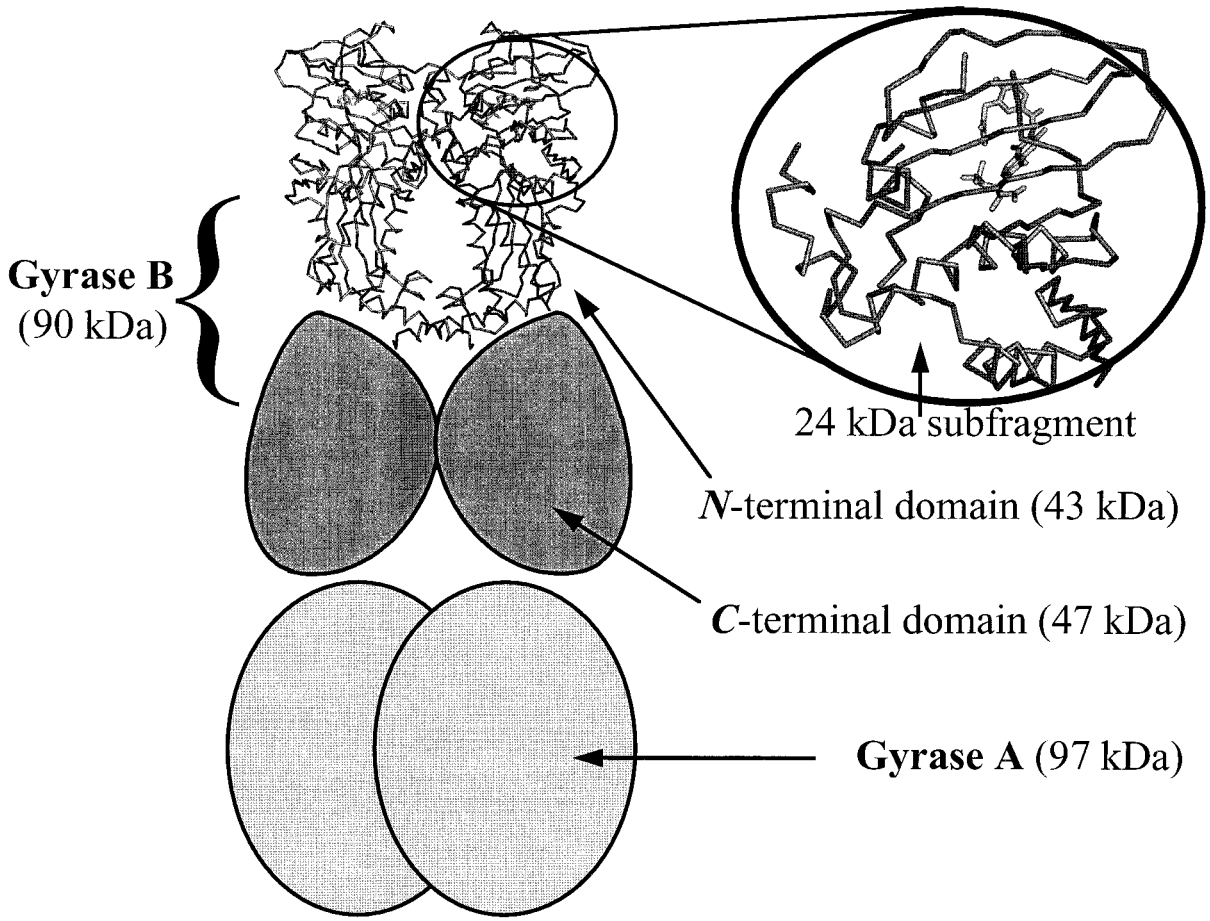

FIGURE 1: Subunit composition and domain structure of DNA gyrase from *E. coli*.

C-terminal subdomain (residues 221−393). Novobiocin is a well-studied coumarin inhibitor of gyrase, and it has been shown that the coumarin binding site lies within the 24 kDa N-terminal subdomain (Gilbert & Maxwell, 1994). Attempts to cocrystallize the 43 kDa fragment with various inhibitors were not met with success, and this led to an exploration of the utility of the N-terminal subdomain. Crystal structures of the 24 kDa fragment complexed with novobiocin as well as other antibiotics have been reported recently (Lewis et al., 1996a,b; Tsai et al., 1997; Pauptit et al., 1997). The insights into gyrase inhibition gleaned from these structures are being exploited in the design of new inhibitors.

Novobiocin prevents dimerization in solution of both the 24 kDa and the 43 kDa fragments (Ali et al., 1993, 1995; Gilbert & Maxwell, 1994). Similarly, the crystal structures of the 24 kDa fragment are monomeric, but many of the residues that bind the adenine moiety to the 43 kDa fragment also interact with novobiocin in the complex with the 24 kDa fragment (Wigley et al., 1991; Lewis et al., 1996a). The coumarin ring replaces the absent Tyr-5′ in a direct interaction with the guanidinium group of Arg-136. This latter residue already was implicated in coumarin binding since nine independent coumarin-resistant isolates of *E. coli* have mutations at Arg-136 (to His, Ser, or Cys; Contreras & Maxwell, 1992). We have used site-directed mutagenesis to prepare the R136H mutant 24 kDa fragment. This mutant was selected because it is the naturally occurring variant which is most closely related to the wild type in terms of side chain character.

We report the energetics of novobiocin binding to the wild type and R136H mutant 24kDa subdomain from the gyrase B subunit. We also present a 2.3 Å crystal structure of novobiocin in complex with the mutant subdomain. This structure has been used, along with empirical relationships, to predict the thermodynamic parameters for the binding of novobiocin. These predictions are interpreted in light of the structural data, and some general conclusions are reached about the role of water molecules in the interface between proteins and their bound ligands.

EXPERIMENTAL PROCEDURES

Materials. The 43 kDa *E. coli* GyrB fragment was prepared as described (Ali et al., 1993) as was the wild-type 24 kDa *E. coli* GyrB fragment (Gilbert & Maxwell, 1994).

Generation of the R136H Mutant. Plasmid pAM24 which encodes the 24 kDa subdomain of GyrB of *E. coli* (Gilbert & Maxwell, 1994) was kindly supplied by A. Maxwell. This was derived from the pAG111 plasmid (Hallett et al., 1990) which carries $lacI^Q$ and *bla*, and in which expression of *gyrB* is driven by p*tac*. Plasmid pAM24 DNA was used as the template in a PCR with two primers (CGTTGATGTC-GAATTCTTATGACTCC and CGTAGATCTGACGGT-GAATTTTACCCTCGTGCTGGAT). This amplified a 440 bp fragment of *gyrB*, including an *Eco*RI site near the start codon through to a *Bgl*II site close to the Arg-136 codon (CGC) which was specifically converted to a His codon (CAC). This fragment was purified, cut with *Eco*RI and *Bgl*II, and then cloned into pAM24 from which the *Eco*RI to *Bgl*II fragment had been excised. After transformation, the desired fragment exchange was confirmed by DNA sequencing. The plasmid encoding the R136H mutant of

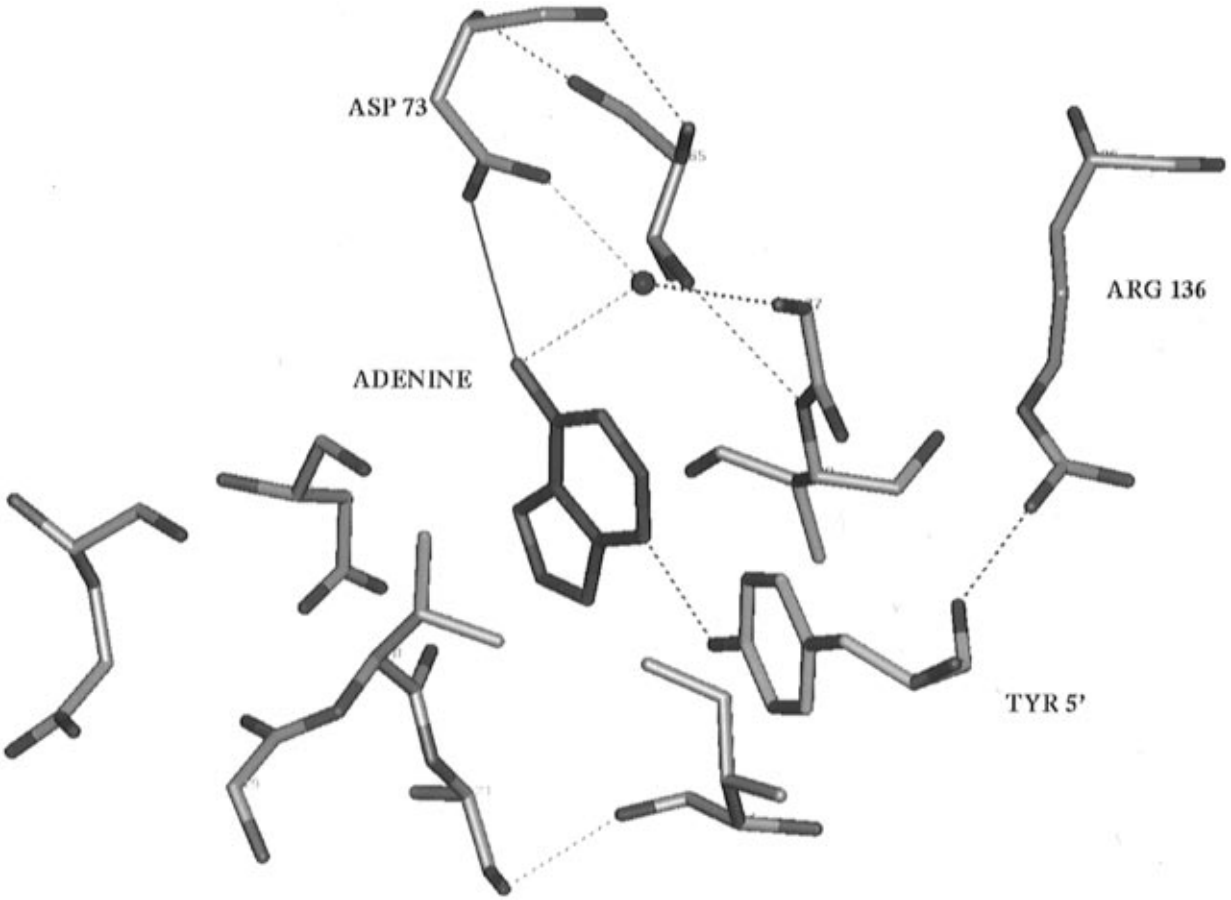

FIGURE 2: Binding site environment of the adenine ring as determined in the complex between ADPNP and the 43 kDa gyrase B subdomain. Adenine carbon atoms are in purple, and those for Tyr-5′ from the N-terminal arm of the other monomer are in yellow. Interactions are indicated by dashed vectors; in particular, the N6 atom of the adenine interacts with the carboxylate of Asp-73, and the aza N3 atom accepts a hydrogen bond from the hydroxyl group of Tyr-5′. The main chain carbonyl oxygen atom of Tyr-5′ interacts with Arg-136.

the 24 kDa GyrB domain (residues 1−220) was designated pTB382 and transformed into *E. coli* MM294.

Protein Expression and Purification. Cultures of this strain were grown at 30 °C with shaking (250 rpm) in L-Broth supplemented with 0.1% glucose and 50 μg/mL ampicillin until the OD_{550} reached 0.45−0.55. At this point, protein expression was induced with 0.5 mM IPTG. Cells were harvested by centrifugation (Sorval RC3B, 5000 rpm., 4 °C, 30 min) 21 h later prior to storage at −80 °C .

Unless otherwise stated, all purification operations were carried out at 4 °C. Cells were suspended (1/4, w/v) in TED buffer [50 mM Tris-HCl (pH 7.4), 1 mM ethylenediaminetetraacetic acid (EDTA), and 5 mM dithiothreitol (DTT)]. Phenylmethanesulfonyl fluoride (PMSF) was added to 50 μM and then lysozyme to 0.2 mg/mL, and the mixture was homogenized for 30 min. The mix then was centrifuged at 40 000 rpm for 1 h, the supernatant retained, and the pellet washed twice with equivalent volumes of TED buffer. The supernatant and washes were combined and mixed with novobiocin−Sepharose overnight. The mixture was packed into a Pharmacia XK column, washed with TED buffer, and eluted, at room temperature, in TED buffer containing 20 mM ATP and 25 mM magnesium acetate. Fractions containing the protein of interest were identified by sodium dodecyl sulfate−polyacrylamide gel electrophoresis (SDS−PAGE), pooled, dialyzed into TED buffer, and loaded onto a Pharmacia Mono Q 10/10 column equilibrated in TED buffer. Protein was eluted on a 0 to 500 mM NaCl/TED gradient. Fractions containing the protein of interest (approximately 150 mM NaCl/TED) were pooled and dialyzed into PED buffer [50 mM sodium phosphate (pH 7.2), 1 mM EDTA, and 5 mM DTT]. The pool was applied to a Pharmacia Mono S 5/5 column equilibrated in PED buffer. The desired protein appeared in the flow through, and bound contaminants were removed from the column with a 1 M NaCl/PED wash. The product, >95% pure by SDS−PAGE and N-terminus sequencing, was confirmed to be [R136H]*E. coli* GyrB (2−220) by electrospray mass spectrometry (MW detected = 24 005.9 Da; theory = 24 007 kDa), N-terminus sequencing, and amino acid analysis.

Isothermal Titration Calorimetry. The binding energetics of novobiocin were measured using an MCS titration calorimeter (MicroCal Inc., Northampton, MA). Proteins were dialyzed exhaustively before titration, and the novobiocin ligand was dissolved in the buffer from the dialysis in order to minimize the heats of dilution when the ligand was injected into the protein solution. Titrations were performed either in 20 mM phosphate buffer (pH 7.4) or in 69 mM Tris-HCl (pH 7.4). Protein concentrations were determined by amino acid analysis. Novobiocin concentrations were measured by absorption at 305 nm.

Figure 3 shows a typical experiment where 72 injections (volume = 3 μL) of 300 μM novobiocin were introduced into the sample cell (volume $\approx$ 1.4 cm^3) containing the His-136 24 kDa fragment (17 μM), while stirring at 400 rpm. The heats of dilution for novobiocin were measured using the same injection protocol, with dialysis buffer replacing the protein solution. These heats were subtracted prior to

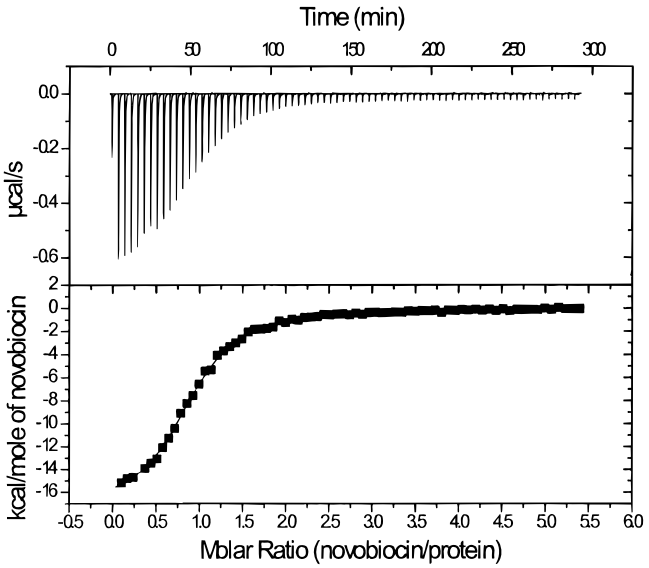

FIGURE 3: Thermogram for the binding of novobiocin to the His-136 24 kDa fragment of gyrase B protein at 300 K in phosphate buffer.

data analysis. Under these conditions, almost all of the novobiocin was bound during the initial injections. Binding caused heat to be released in the sample cell, and power was applied to the reference cell until the desired temperature difference was regained. The power against time plot (Figure 3, upper panel) shows a peak as heat is released upon binding following the injection and then returns to the baseline as thermal equilibrium is reached. The area under the peak gives the amount of heat released (Figure 3, lower panel). The data were analyzed using MicroCal Origin software which included corrections to allow for the volume changes during each injection [see Wiseman et al. (1989) and Bundle and Sigurkjold (1994)]. These procedures assumed a simple-single site binding model and allowed estimation of K_a ($=1/K_d$), $\Delta H°$, and the number of moles of ligand bound per mole of protein, n. The solid line in Figure 3 (lower panel) is the theoretical binding isotherm with the parameter values given in Table 1. Since

$$RT \ln K_d = \Delta G° = \Delta H° - T\Delta S° \qquad (1)$$

these data allow calculation of $T\Delta S°$. The degree of precision in calorimetric measurements was dependent upon the magnitude of $\Delta H°$ and the amount of protein in the cell. For these experiments, a change in $\Delta G°$ or $\Delta H°$ of 1 kcal/mol was regarded as significant, whereas a larger change of 2 kcal/mol was required for significance in $T\Delta S°$ because this parameter was calculated as the difference between $\Delta G°$ and $\Delta H°$.

In this range, the value of $\Delta H°$ approximates to a linear function of T where

$$\Delta C_p = (\Delta H°_{T_2} - \Delta H°_{T_1})/(T_2 - T_1) \qquad (2)$$

and ΔC_p is the change in heat capacity at constant pressure upon binding. This relationship allowed calculation of ΔC_p from measurements of $\Delta H°$ at different temperatures.

Crystallization. The complex beteween novobiocin and the mutated gyrase fragment was crystallized by the hanging drop vapor diffusion method using a reservoir consisting of 12% (v/v) polyethylene glycol 200 (PEG 200) and 100 mM MES (pH 6.0 or 6.2). Drops were formed by mixing equal amounts of protein/novobiocin (12 mg/mL) and reservoir solutions on siliconized glass coverslips and allowed to equilibrate with the reservoir solution in sealed wells of a Linbro plate at 20 °C. Needle-shaped crystals grew over a period of 7−10 days to an approximate maximum size of 0.6 mm × 0.04 mm × 0.04 mm.

Crystallographic Data Collection, Processing, and Model Refinement. Data were collected on station 9.6 of the synchrotron radiation source at Daresbury Laboratory (Daresbury, Cheshire, U.K.). A single crystal was transferred to a solution of 30% (v/v) PEG 200 for 2 min, suspended in a fiber loop, and flash-frozen at 100 K, using an Oxford Cryosystems Cryostream cooler. A 30 cm MarResearch image plate detector was used to collect 134 rotation images of 1° crystal rotation each at a crystal to detector distance of 300 mm. The wavelength of the source was 0.87 Å, and diffraction to approximately 2.1 Å was observed.

Data were processed using the MOSFLM software suite adapted for use with image plate data (A. Leslie, personal communication). The crystals were isomorphous with respect to those of the wild-type novobiocin−24 kDa fragment complex, being of space group $P2_12_12_1$ with a = 39.5 Å, b = 47.7 Å, and c = 114.4 Å. Orientation matrices were determined using reflections located in 5° phi wedges starting at 0, 30, 60, and 90° and subsequently used in postrefinement (using the POSTREF SEGMENT keyword in MOSFLM). The orientation parameters obtained following convergence of postrefinement were fixed during the subsequent profile fitting and integration. Batches of integrated intensities were scaled together using programs ROTAVATA and AGROVATA and converted to structure factor amplitudes using the program TRUNCATE (CCP4, 1994). The final data consist of 9455 unique reflections (from 48 291 measurements) with an R_{sym} of 0.065 and an overall completeness and multiplicity of 94.8% and 5.1, respectively, to 2.3 Å. Data beyond 2.3 Å were considered too weak for inclusion in the final data set. Data collection statistics are presented in Table 2.

Model building was initiated using the protein model (with Arg-136 excised) from the 24 kDa gyrase B−novobiocin complex (Pauptit et al., 1997), which was used to phase $2F_o - F_c$ and $F_o - F_c$ difference Fourier syntheses. The inital R-factor and free R-factor were 0.274 and 0.400, respectively. Refinement of the protein model alone with XPLOR (Brünger et al., 1987) started with rigid body refinement to compensate for any slight nonisomorphism between wild-type and mutant protein crystals. Thereafter, a single group temperature factor decrement (to be applied to all individual model temperature factors) was refined, since the data were collected at low temperature but the model temperature factors originated from a room-temperature experiment. This was followed by standard simulated annealing. After rebuilding with O (Jones et al., 1991), the ligand was modeled into clear difference density and refinement continued using the conjugate direction method of TNT (Tronrud et al., 1987) with temperature factor correlation restraints applied. Water molecules were added to the refined model only if their presence was indicated by both $2F_o - F_c$ and $F_o - F_c$ maps and they could participate in hydrogen bonds. They were subsequently retained only if their temperature factor remained below 40 Å^2 upon refinement.

Table 1: Thermodynamic Parameters for the Interaction of Novobiocin with Fragments of the DNA Gyrase B Protein[a]

protein	buffer	temperature (K)	K_d (nM)	$K_a \times 10^{-6}$ (M^{-1})	$\Delta G°$ (kcal/mol)	$\Delta H°$ (kcal/mol)	$T\Delta S°$ (kcal/mol)	stoichiometry
24 kDa	phosphate	300	32 ± 3	31 ± 2	−10.3 ± 0.1	−12.1 ± 0.1	−1.8 ± 0.1	1.2 ± 0.1
24 kDa	Tris	300	43 ± 7	23 ± 4	−10.1 ± 0.1	−12.2 ± 0.1	−2.1 ± 0.2	1.3 ± 0.1
43 kDa	phosphate	300	26 ± 3	38 ± 5	−10.4 ± 0.1	−12.7 ± 0.1	−2.3 ± 0.1	1.1 ± 0.1
43 kDa	Tris	300	18 ± 5	56 ± 15	−10.6 ± 0.1	−10.7 ± 0.1	−0.1 ± 0.1	1.3 ± 0.1
24 kDa	phosphate	282	28 ± 3	36 ± 4	−9.8 ± 0.1	−8.7 ± 0.1	1.1 ± 0.1	1.0 ± 0.1
24 kDa	phosphate	292	46 ± 5	22 ± 2	−9.8 ± 0.1	−11.1 ± 0.1	−1.3 ± 0.1	1.0 ± 0.1
24 kDa	phosphate	305	92 ± 7	11 ± 1	−9.8 ± 0.1	−15.5 ± 0.1	−5.6 ± 0.1	1.0 ± 0.1
24 kDa	phosphate	310	130 ± 10	7.8 ± 0.7	−9.8 ± 0.1	−17.0 ± 0.1	−7.3 ± 0.2	1.0 ± 0.1
24 kDa His-136	phosphate	300	1200 ± 100	0.82 ± 0.02	−8.1 ± 0.1	−17.5 ± 0.1	−9.3 ± 0.1	0.9 ± 0.1
24 kDa His-136	Tris	300	1200 ± 50	0.83 ± 0.03	−8.1 ± 0.1	−14.3 ± 0.1	−6.1 ± 0.1	0.9 ± 0.1
24 kDa His-136	phosphate	285.5	600 ± 50	1.7 ± 0.1	−8.1 ± 0.1	−10.0 ± 0.1	−1.9 ± 0.1	1.1 ± 0.1
24 kDa His-136	phosphate	296	980 ± 40	1.0 ± 0.1	−8.2 ± 0.1	−14.7 ± 0.1	−6.5 ± 0.1	0.8 ± 0.1
24 kDa His-136	phosphate	305	2000 ± 100	0.49 ± 0.01	−7.9 ± 0.1	−18.0 ± 0.1	−10.1 ± 0.1	1.0 ± 0.1
24 kDa His-136	phosphate	310	3600 ± 200	0.28 ± 0.02	−7.7 ± 0.1	−21.5 ± 0.4	−13.8 ± 0.4	1.0 ± 0.1

[a] The binding energetics were measured by isothermal titration calorimetry as described in Experimental Procedures. Values of K_a, $\Delta G°$, $\Delta H°$, and $T\Delta S°$ relate to association. The values of the dissociation constant, K_d ($=1/K_a$), also are shown and they indicate the concentration of novobiocin free in solution when binding reaches 50% saturation. The standard error for some entries has been estimated where the values from the fitting procedure (see Experimental Procedures) are unreasonably small.

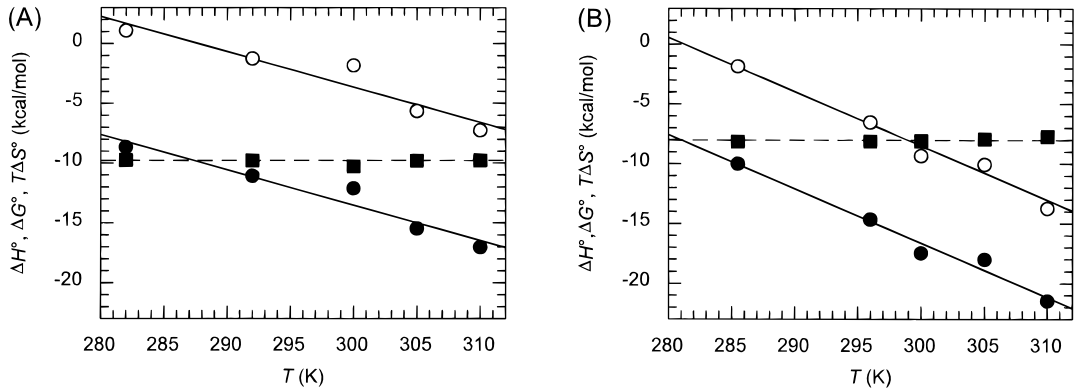

FIGURE 4: Temperature dependence of novobiocin binding energetics. The lines were drawn using the parameter values in Tables 1 and 3. The solid lines describe the temperature dependence of $\Delta H°$ (filled circles) and $T\Delta S°$ (open circles). The dashed line shows that for $\Delta G°$ (squares), which was assumed to be constant: (A) the wild-type 24 kDa fragment and (B) the His-136 24 kDa fragment.

Thermodynamic Parameter Prediction Methods. Accessible surface areas were estimated using the program SAREA (Pearlman, 1982), with standard atomic radii (Lee & Richards, 1971). The following relationships at 300 K were generated from empirical equations (Gomez & Freire, 1995)

$$\Delta C_p = 0.4383\Delta\mathrm{ASA}_{ap} - 0.2694\Delta\mathrm{ASA}_{pol}\ \mathrm{cal\ K^{-1}\ mol^{-1}} \quad (3)$$

$$\Delta H° = 0.0403\Delta\mathrm{ASA}_{pol} - 0.0229\Delta\mathrm{ASA}_{ap}\ \mathrm{kcal/mol} \quad (4)$$

$$T\Delta S° = 0.02019\Delta\mathrm{ASA}_{pol} - 0.03285\Delta\mathrm{ASA}_{ap}\ \mathrm{kcal/mol} \quad (5)$$

where $\Delta\mathrm{ASA}_{ap}$ and $\Delta\mathrm{ASA}_{pol}$ are the changes in apolar and polar accessible surface areas (in Å^2), respectively, calculated as that in the complex minus that when free. It was assumed that the nonbound conformations of the interacting partners are the same as those in the complexes.

RESULTS

Energetics of Novobiocin Binding to Fragments of the Gyrase B Protein. Isothermal titration calorimetry was used to characterize the binding of novobiocin to fragments of the *E. coli* gyrase B protein (Table 1). The stoichiometry is close to 1 in all cases, indicating that most of the protein in these samples is active. Titrations were performed in phosphate and Tris buffers, which have enthalpies of ionization (proton release) of around +0.8 and +11.3 kcal/mol, respectively. Thus, $\Delta H°$ is expected to be 10.5 kcal/mol more positive in Tris if the association of novobiocin with the protein involves the net uptake of one proton. The observed change in $\Delta H°$ is −0.1 kcal/mol for the 24 kDa fragment, +2.0 kcal/mol for the 43 kDa protein, and +3.2 kcal/mol for the 24 kDa R136H fragment. These results imply that, if there is any net proton movement, it involves a partially ionized group. Thus, the values measured in phosphate are unlikely to be affected significantly by net proton movement, and the protonation state of His-136 is not known.

Novobiocin has similar affinities and energetics for binding to the 24 and 43 kDa fragments (Table 1), suggesting that it forms similar interactions with the two proteins. At 300 K, the K_d is around 28 nM with $\Delta H°$ being favorable and $T\Delta S°$ being unfavorable. Our values for the energetics of binding to wild-type fragments are in close agreement with those previously published (Gormley et al., 1996; Tsai et al., 1996). Binding to the R136H mutant 24 kDa fragment leads to an increase in K_d to 1200 nM. $\Delta H°$ becomes 5.4 kcal/mol more favorable, and $T\Delta S°$ is 7.6 kcal/mol less favorable (Table 1).

The temperature dependence of novobiocin binding to the wild-type and mutant 24 kDa fragments also was investigated (Figure 4 and Table 3). Although the $\Delta G°$ values are remarkably constant, there are substantial differences in the

Table 2: X-ray Data Collection and Refinement Statistics for the R136H Mutant 24 kDa Subdomain of the DNA Gyrase B Protein[a,b]

Crystallographic Data	
space group (number)	$P2_12_12_1$ (19)
unit cell (Å) (*a*, *b*, and *c*)	39.50, 47.72, 114.41
resolution of data (Å)	2.3
no. of measurements	48291
no. of unique reflections	9455
multiplicity	5.1 (5.2)[a]
completeness (%)	94.8 (97.0)[a]
R_{symm}	0.065 (0.131)[a]
$I/\sigma(I)$	8.5 (5.6)[a]
Final Model Statistics	
R-factor	0.195 (0.230)[b]
free *R*-factor	0.299 (0.132)[b]
rmsd from ideality for bond lengths (Å)	0.012
rmsd from ideality for bond angles (deg)	1.3
average main chain temperature factor (Å^2)	20.0
average side chain temperature factor (Å^2)	25.4
average water temperature factor (Å^2)	31.0

[a] Figures in parentheses refer to outer shell (2.38−2.30 Å). [b] Figures in parentheses refer to outer shell (2.4−2.3 Å).

individual enthalpic and entropic contributions. For example, at 282 K, the binding of novobiocin to the wild-type protein is both enthalpically and entropically favored, whereas at 310 K, the binding is enthalpically driven and must overcome an unfavorable entropy. This is as an example of enthalpy−entropy compensation, which is common in biomolecular interactions because favorable changes in $\Delta H°$ are linked with an entropic cost (Dunitz, 1995; Grunwald & Steel, 1995). The favorable entropy change at low temperatures probably occurs because the effects of the release of bound water outweigh the cost of the increase in intrinsic order arising from complex formation.

The magnitudes of $\Delta H°$ and $\Delta S°$ are a function of ΔC_p, which may be calculated directly from the observed change in $\Delta H°$ with temperature. ΔC_p itself may change with temperature (Liu & Sturtevant, 1995). There is some curvature in a plot of $\Delta H°$ against T for the wild-type 24 kDa protein (Figure 4A). Fitting of a polynomial curved function to these data gives a ΔC_p of -311 cal mol^{-1} K^{-1} at 298 K. Application of an F test (Mannervik, 1982) to compare the residual sum of squares for polynomial *versus* linear fitting indicates that ΔC_p does not change significantly with temperature for these data. Thus, a simple linear model (eq 2) gives the best estimate of $\Delta C_p = -(295 \pm 24)$ cal mol^{-1} K^{-1}. There is no obvious curvature for the plot of $\Delta H°$ against T for the mutant protein (Figure 4B), allowing calculation of a ΔC_p of $-(454 \pm 38)$ cal mol^{-1} K^{-1}.

Structure of the R136H 24 kDa Fragment Complexed with Novobiocin. The refined model of 1592 atoms consists of 194 amino acids, one novobiocin molecule, and 89 water molecules. As with the wild-type fragment (Pauptit et al., 1997), there are disordered loops and termini. The model of the complex between the mutant gyrase fragment and novobiocin consists of residue segments 12−82, 88−104, and 112−217, whereas for the wild-type complex, the modeled segments were 17−80, 90−100, and 116−218. The final crystallographic *R*-factor and free *R*-factor are 19.5 and 29.9%, respectively. Average and root mean-squares values of temperature factors for the various segments of the model are given in Table 2. The stereochemical quality of the model is good; for 162 residues that are non-glycine, non-proline, and nonterminal, 149 (92%) are in the most favored regions of the Ramachandran plot as determined by PROCHECK (Laskovski et al., 1993). Only one residue (Asn-178) is in a disallowed region, and this adopts a classical C_7 axial conformation normally associated with glycine residues. For bond lengths and angles, rms deviations from ideality are low (Table 2).

The overall fold of the mutant (2.3 Å resolution) and wild-type (2.5 Å resolution) models is the same; the rms deviation of 172 corresponding α-carbon atoms is 0.55 Å. The novobiocin molecules superimpose very closely. When compared to the clorobiocin complex (2.1 Å resolution; Tsai et al., 1997), a closer agreement is seen, probably reflecting the greater accuracy of the mutant and the clorobiocin complex structures relative to the wild-type novobiocin structure (the rms deviation of 172 common α-carbon atoms is lower at 0.38 Å). There is only one significant difference in the main chain conformation, a 1.36 Å shift of the α-carbon away from the novobiocin molecule at residue 136, the site of the mutation. We suggest that this is a consequence of the loss of the Arg-136−novobiocin interaction. Minor main chain differences are confined to loop regions. Similarly, differences in side chain conformations are confined to surface residues that are not involved in symmetry contacts.

The novobiocin binding site in the mutant structure is illustrated in Figure 5, and Figure 6 shows the environment of residue 136 in the wild-type and mutant structures. In the wild-type structure, Arg-136 forms a direct hydrogen-bonding interaction with novobiocin; the coumarin carbonyl oxygen is 3.03 and 2.63 Å from the guanidinium Nη_1 and Nη_2, respectively. In contrast, the mutant structure shows no direct interactions between His-136 and the coumarin ring. The histidine side chain was clearly resolved in the initial Fourier maps (Figure 7). The electron density indicates, persistently after several omit map/refinement cycles, that the His-136 imidazole ring should be modeled with an unfavorably planar χ_2 angle of −171°, whereas the preferred rotamers would have values of ±90°. This eclipsed conformation is rare but not unprecedented (see, for example, His-57 in 2MHR, His-B257 in 5RUB, and His-443 in 1GPB, where 2MHR, etc., are Brookhaven Protein Data Bank accession codes) and appears to be stabilized by a hydrogen-bonding interaction between His-136(Nδ_1) and the main chain carbonyl moiety of Arg-76 (2.9 Å), as well as a weaker interaction between His-136(Nϵ_2) and Thr-80(O$_\gamma$) (3.0 Å).

The volume vacated by the guanidinium group contains an ordered water molecule ($B = 26$ Å^2) in the mutant (Figure 8). This water molecule forms hydrogen bonds with a coumarin carbonyl oxygen on the ligand (2.8 Å) and with the carbonyl oxygen of Gly-77 on the protein (3.0 Å). It is 3.5 Å away from His-136(Nδ_1), which is too far to be considered a direct interaction.

DISCUSSION

Affinity of Novobiocin for Different Fragments. Of concern was the fact that the isolated protein fragments used in this study might behave differently with respect to the same regions when located in the intact gyrase tetramer. However, the measured K_d values around 30 nM for the wild-type 24 and 43 kDa proteins (Table 1) are similar to the K_i values of 6−10 nM for novobiocin inhibiting the DNA

Table 3: Comparison of Observed Experimental and Predicted Thermodynamic Binding Data[a]

PDB[b] code	protein	ligand	ΔASA_{ap} (Å^2)	ΔASA_{pol} (Å^2)	waters[c]	ΔC_p (cal mol^{-1} K^{-1}) observed	ΔC_p predicted	$\Delta\Delta C_p$/water	$\Delta H°$ (kcal/mol) observed	$\Delta H°$ predicted	$\Delta\Delta H°$/water	$T\Delta S°$ (kcal/mol) observed	$T\Delta S°$ predicted	$T\Delta\Delta S°$/water
g24[e]	gyrase 24 kDa fragment	novobiocin	−486	−370	3	−295	−113	−61	−12.1	−3.8	−2.8	−1.8	+8.5	−3.4
m24[e]	gyrase 24 kDa fragment His-136	novobiocin	−461	−344	4	−454	−109	−86	−17.5	−3.3	−3.6	−9.4	+8.2	−4.4
5cna[f]	concanavalin A	methyl α-D-mannoside	−142	−246	3	−48	+4	−17	−7.1	−6.7	−0.1	−2.1	−0.3	−0.6
1rob[g]	ribonuclease A	2′-CMP	−149	−400	6	−210	+43	−42	−14.7	−12.7	−0.3	−6.6	+3.2	−1.6
1fkb[h]	FKBP	rapamycin	−539	−419	5	−358	−123	−47	−20.0	−4.5	−3.1	−7.3	+9.2	−3.3
2fke[i]	FKBP	FK506	−555	−345	5	−291	−150	−28	−17.2	−1.2	−3.2	−4.9	+11.3	−3.2
2wrp[j]	*trp* repressor	tryptophan	−310	−218	6	−230	−77	−26	−12.8	−1.7	−1.9	−7.0	+5.8	−2.1
4ape[k] 4er2[l]	endothiapepsin[d]	pepstatin	−774	−513	5	−310	−217	−21	−4.1	−1.8	−0.5	+5.0	+1.1	−0.8
1hah[m]	thrombin	Na^+	−8	−166	10	+1100	+41	−106	−14.2	−7.4	−0.7	−12.3	−3.1	−0.9

[a] Data relate to 298 K, except for gyrase (300 K) and endothiapepsin (289 K). References for thermodynamic data are as follows: gyrase, current work; concanavilin A and ribonuclease A, Chervenak and Toone (1994); FKBP, Connelly et al. (1993); *trp* repressor, Hu and Eftink (1994); endothiapepsin, Gomez and Freire (1995); thrombin, Guinto and Di Cera, (1996). [b] PDB, Protein Data Bank (Bernstein et al., 1977). [c] Number of water molecules involved in bridging between ligand and protein. [d] Entry 4ape is the free protein, and 4er2 is the complex. [e] This work. [f] Naismith et al. (1994). [g] Lisgarten et al. (1993). [h] Van Duyne et al. (1991). [i] Becker et al. (1993). [j] Lawson et al. (1988). [k] Blundell et al. (1990). [l] Bailey et al. (1993). [m] Vijayalakshmi et al. (1994).

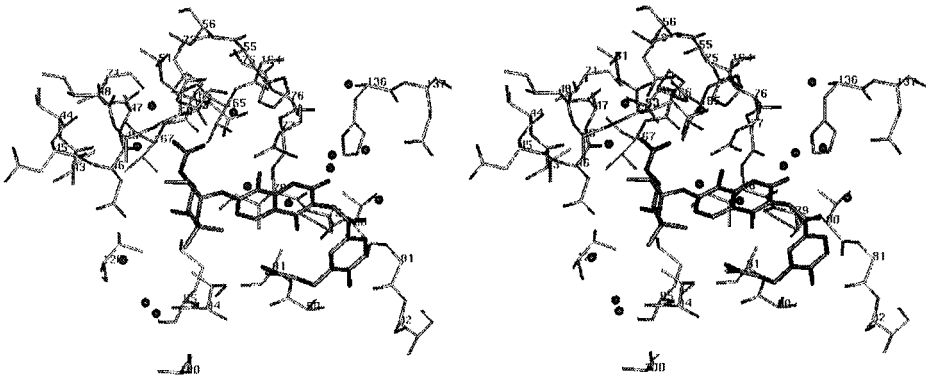

FIGURE 5: Stereopair (relaxed eye) diagram of the novobiocin binding site in the R136H mutant 24 kDa subdomain of DNA gyrase B. All residues within 7 Å of novobiocin are included with water molecules represented as spheres.

supercoiling and DNA-dependent ATPase activities of intact *E. coli* gyrase (Sugino et al., 1978). Thus, direct calorimetric measurement of binding to fragments is in agreement with the relatively indirect kinetic measurements on the intact protein. This suggests that these fragments have similar structural and functional characteristics when included in the intact gyrase molecule.

Novobiocin has similar K_d values for the 43 and 24 kDa wild-type fragments (Table 1). Conversely, the affinity for the His-136 mutant is reduced 38-fold to a K_d of 1200 nM. In *E. coli*, the mutation is associated with a 12-fold increase in IC_{50} from 50 to 580 μg of novobiocin/mL (Contreras & Maxwell, 1992). Increased expression of the mutant gyrase due to reduced catalytic activity may contribute to the apparently smaller change *in vivo*. The reduced affinity displayed by the mutant protein suggests that interactions made by Arg-136 are important.

Structure of the Mutant Complex. Both the wild-type and mutated 24 kDa fragment structures contain a number of flexible loops which probably arise due to isolation from the rest of the gyrase molecule. The mutant model represents a higher-resolution novobiocin complex than the wild-type structure. As in the wild-type structure, the novobiocin adopts a conformation with a cis peptide between the coumarin ring and the hydroxybenzoate such that hydrophobic portions of the molecule cluster with hydrophobic residues in the protein. This is known not to be an artifact induced by the lattice contacts formed by novobiocin, since the same conformation is detected in solution by NMR (Tsai et al., 1997). The bound conformation is strikingly different from the isolated novobiocin crystal structure (Boles & Taylor, 1995; Allen & Kennard, 1993), which has a planar extended conformation with a trans peptide. In the mutant gyrase fragment complexed with novobiocin, the structural model refines equally well when the cis peptide is restrained to be planar as when these restraints are released. Thus, protein crystallography gives no strong support for a nonplanar peptide as has been proposed (Brand & Toribara, 1972) to account for spectroscopic data. The suggested lack of conjugation across this peptide may be satisfied as long as the peptide is not coplanar with the coumarin and in the case of the bound cis conformation there is no such coplanarity.

The two main differences between the structures of the mutant and wild-type complexes involve a relatively strained conformation for His-136 and the presence of a sequestered water in the volume vacated by the guanidinium group that arises from the replacement of the Arg (Figure 6).

Change in Heat Capacity on Complexation. Studies of thermally induced protein unfolding using differential scanning calorimetry show that the magnitude of ΔC_p is linearly dependent upon the change in solvent accessible surface area.

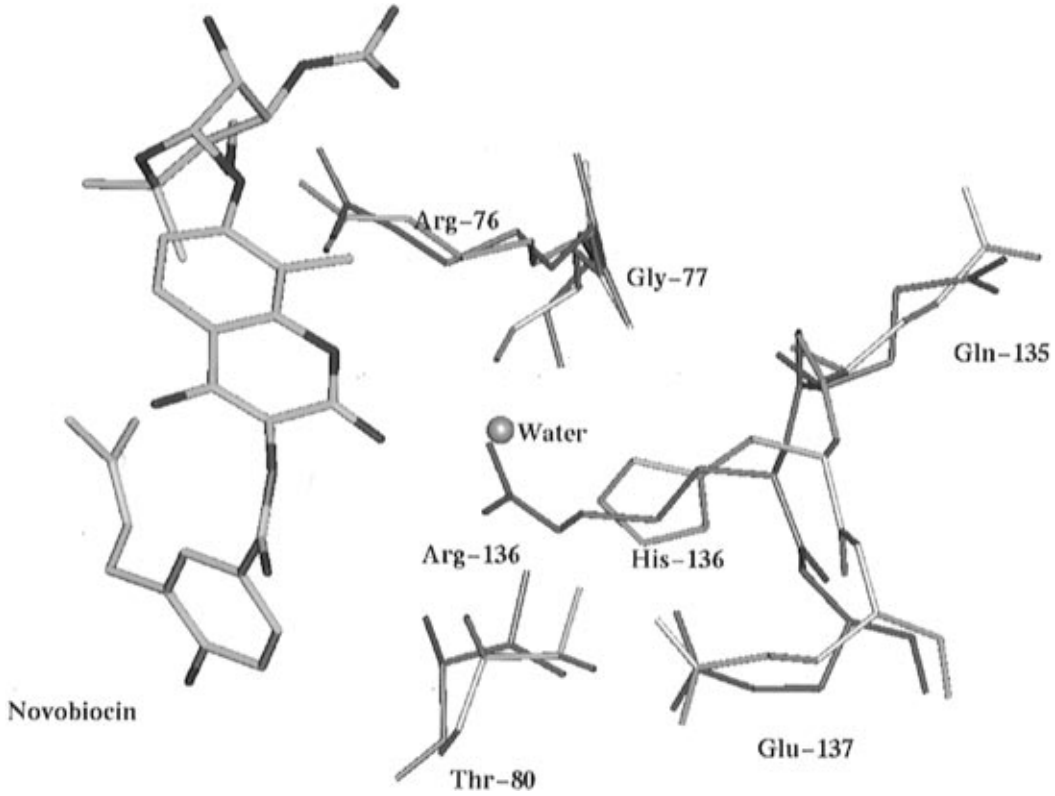

FIGURE 6: Interactions between wild-type and mutant 24 kDa fragments from the *E. coli* gyrase B protein and novobiocin. The wild-type protein is in pink, and the mutant protein and sequestered water are in blue. Novobiocin carbon atoms are in yellow. Note the cis peptide bond in novobiocin and the correspondence between the water position in the complex with the mutant protein and the guanidinium group of the wild type. The significant displacement of the main chain in the region of residues 135−137 can also be seen.

For protein unfolding, accessible surface area increases, whereas generally for ligand binding, there is a decrease in solvent accessible surface area. The increase in solvent accessibility for apolar surfaces in protein unfolding results in the major, positive contribution to ΔC_p, whereas the increase in accessibility of polar surfaces gives rise to smaller negative factors (eq 3; Spolar et al., 1989; Freire, 1994). Since for ligand binding solvent accessible area decreases, the data from protein unfolding studies predict a major negative contribution to ΔC_p due to the burial of apolar surface and a small positive contribution arising from the decrease in solvent accessibility of polar surfaces. The changes in accessible surface area which occur on ligand binding, however, are likely to be much smaller so that groups which make an unusual contribution could have a relatively larger effect.

The ΔC_p on binding of novobiocin is negative for both 24 kDa fragments, with the mutant protein exhibiting a much larger value (Table 3 and Figure 4). Such a large negative shift in ΔC_p could thus reflect significant changes in conformation leading to burial of a greater hydrophobic surface area. For this system, X-ray crystallography indicates that this is not the explanation (Figure 6). Furthermore, compared to the wild-type, binding to the mutant protein at 300 K is enthalpically more favored, and there is a less favorable entropic contribution (Table 1). These shifts are the opposite of those expected from an increased hydrophobic contribution.

Prediction of Binding Energetics. The three-dimensional crystal structures of the wild-type and R136H mutant complexes allow calculation of ΔASA_{ap} and ΔASA_{pol} (Table 3). When the thermodynamic parameters estimated using the empirical relationships (eqs 3−5) are compared to those determined experimentally (Table 3), there is a striking lack of agreement. ΔC_p and $\Delta H°$ are significantly underestimated, and the calculated $T\Delta S°$ values have the wrong sign. The large differences between mutant and wild-type proteins are not reproduced by the empirical calculations, and the source of these discrepancies is suggested by examination of the crystal structures of the complexes.

The relatively strained conformation of His-136 seems to be unlikely to contribute significantly to the energetic cost observed in the binding of novobiocin to resistant gyrase. This conformational strain is compensated for by hydrogen bonds to a main chain carbonyl and a threonine side chain, and the histidine does not participate directly in the protein−ligand interface. Although no structure is available for the uncomplexed protein, it seems likely that the conformation of His-136 will be the same in both free and bound states and thus will not affect the energetics of binding.

Contribution of Sequestered Water to the Binding Energetics. The most obvious change in the structures upon mutation (Figure 8) is the sequestration of a water molecule into the volume vacated by the removal of the guanidinium group. This water links the novobiocin to atoms in the mutant protein *via* hydrogen bonds. It seems that the more negative ΔC_p arises from this sequestered water. Previously published data show a similar influence of the immobilization of water at the binding interface (Table 3). Ladbury et al. (1994) highlight the fact that the ΔC_p on formation of the *trp* repressor−operator complex is much more negative than might be expected, and the binding of a sodium ion to thrombin also has a large negative ΔC_p (Guinto & Di Cera, 1996). Similar effects have been observed for lysozyme−

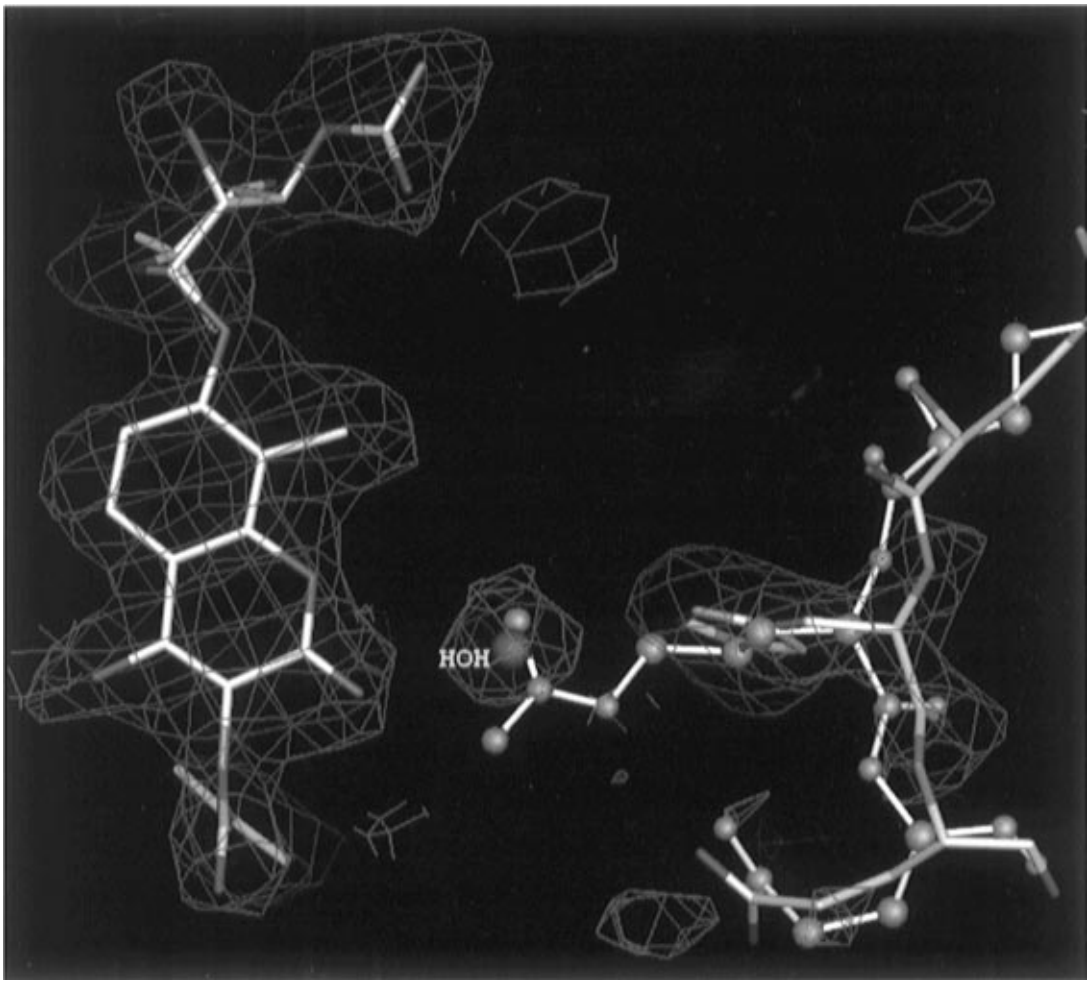

FIGURE 7: Electron density omit map for the R136H mutant 24 kDa subdomain of DNA gyrase B, omitting residue 136, novobiocin, and localized water. The region of residues 135−137 is shown in element colors for the mutant and pink for the wild-type protein. The fit to the density of novobiocin can be seen along with the water position labeled in yellow.

antibody complexes (Schwarz et al., 1995). These results were interpreted as suggesting that sequestration of waters into a more ordered structure within the interface results in a lower heat capacity compared to those which are on the surface or in bulk solution. It has been argued that the increased order leads to stiffer internal modes of vibration which generate negative contributions to ΔC_p and $T\Delta S°$ (Sturtevant, 1977). If it is assumed that sequestration of water is one of the major causes of inaccuracy in the predicted ΔC_p values (Table 3), then trapping of each water molecule makes the observed ΔC_p more negative than the predicted value by approximately 48 ± 31 cal K^{-1} mol^{-1}. This range agrees with data on the dissolution of diketopiperazine crystals, which suggest a ΔC_p of −60 ± 8 cal K^{-1} mol^{-1} for the sequestration of a water molecule (Haberman & Murphy, 1996). A similar analysis for the *trp* repressor−operator and MetJ−metbox interactions suggests that the approximate contribution to ΔC_p for each water molecule immobilized at the interface is −6 and −12 cal K^{-1} mol^{-1}, respectively (Morton & Ladbury, 1996). These values represent smaller contributions than that for the single water molecule under consideration in the mutant gyrase fragment−novobiocin complex. This may arise because the protein−DNA systems reflect the averages for large numbers of water molecules, some of which will make weaker or fewer hydrogen bonds than for the water considered here (J. E. Ladbury, personal communication).

The observed change in $\Delta G°$ of 2.2 kcal/mol (Table 1), when comparing binding of novobiocin to the wild-type and mutant gyrase fragments, reflects both the loss of hydrogen bonding from Arg-136 and the gain of hydrogen bonds involving the sequestered water. These new interactions may explain why this value is at the low end of the range quoted for hydrogen bonds involving charged groups (Fersht et al., 1993). The mutation R136H causes a favorable change in $\Delta H°$ of 5.4 kcal/mol and an unfavorable change in $T\Delta S°$ of 7.6 kcal/mol (Table 1). Both of these shifts are in the direction opposite to that expected for a mutation which removes a key hydrogen-bonded interaction to a side chain, and they presumably reflect the effects of water sequestration into the binding interface.

Comparisons of observed and expected $\Delta H°$ and $T\Delta S°$ values for a range of protein−ligand interactions (Table 3) imply that the incorporation of a water molecule has approximately equal effects on these parameters, each being changed by around −1 to −3 kcal mol^{-1} $water^{-1}$. Hilser et al. (1996) estimate an enthalpic contribution of −0.5 kcal mol^{-1} $water^{-1}$ from data on lysozyme−antibody complexes (Bhat et al., 1994). Thus, the immobilized waters generate a largely compensated, minor contribution to $\Delta G°$ around 300 K. Similar effects may be anticipated for water molecules immobilized on complex formation and which interact with either the protein or ligand alone.

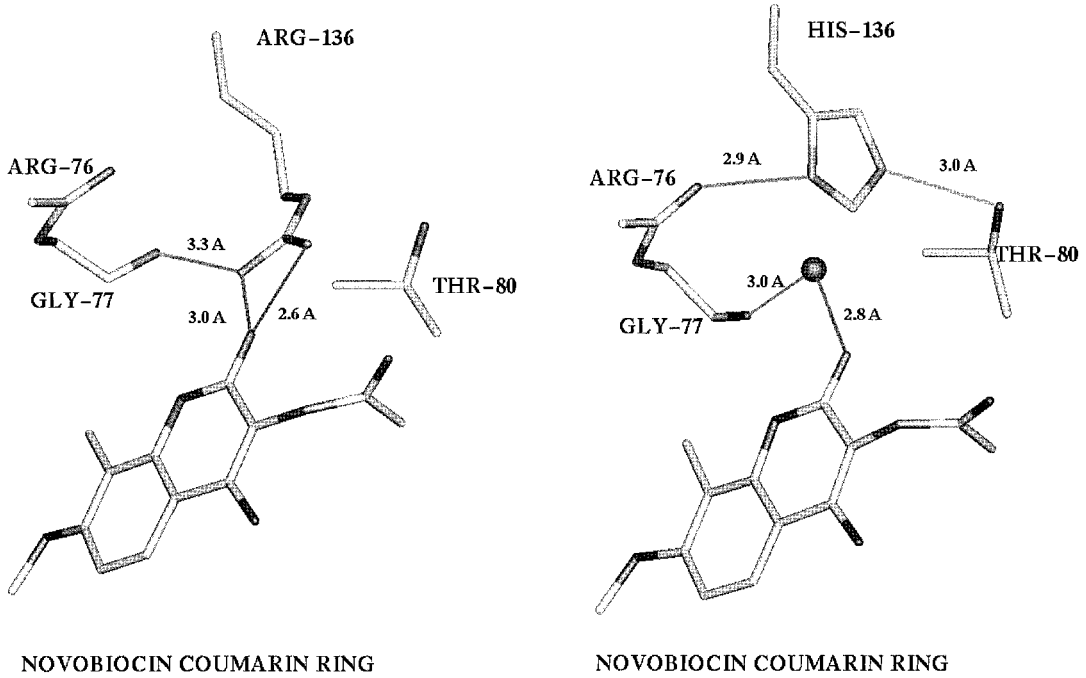

FIGURE 8: Comparison of the hydrogen bonding environment for the coumarin ring of novobiocin in wild-type (left) and R136H (right) 24 kDa fragments from the *E. coli* gyrase B protein.

The variation in the estimates of the effects of sequestered waters may reflect the importance of the particular environment in addition to uncertainties in structural and thermodynamic data. This contribution of sequestered water in protein−protein, protein−DNA, and protein−ligand complexes introduces difficulties into the interpretation of thermodynamic data, especially in the absence of structural information. The use of negative changes in ΔC_p in diagnoses of the extent of nonpolar surface buried appears to be unreliable. Also, although changes in $\Delta H°$ and $T\Delta S°$ may arise largely from solvent contributions, these factors compensate in their contribution to $\Delta G°$ which will thus tend to reflect changes in direct interactions. Similar large changes in $\Delta H°$, which are not reflected in changes in $\Delta G°$ due to enthalpy−entropy compensation, are highlighted in the binding of barnase and barstar mutants (Frisch et al., 1997).

Gomez and Freire (1995) find good agreement between observed and predicted energetics for the interaction between endothiapepsin and pepstatin. Unlike the current work (Table 3), they treat the hydroxyl groups of Ser and Thr as groups making a negative contribution to ΔC_p of dehydration, which is normally a characteristic of a hydrophobic group. It seems possible that solvation effects may contribute to the unexpected energetic contributions of Ser and Thr residues.

This study has implications for the rational design of ligands that bind to proteins. The replacement of ordered water in a protein−ligand interface can lead to tighter binding. This has been exploited in the design of HIV protease inhibitors (Lam et al., 1994), and the current work illustrates that changing from mutant to wild-type gyrase, replacing an ordered water molecule by a guanidinium group, gives rise to a 38-fold increase in affinity for novobiocin. In competition binding assays, clorobiocin appears to have an affinity approximately 6-fold higher than that of novobiocin for the 24 and 43 kDa fragments (Gormley et al., 1996). This could reflect the observed displacement of ordered water from the protein−ligand interface when the carbamoyl group is replaced by the larger acyl-pyrrole moiety of clorobiocin (Lewis et al., 1996a; Tsai et al., 1997).

Following similar observations, Ladbury and Chowdhry (1996) have suggested the designed incorporation of hydrogen-bonding water molecules into the interface between candidate ligand and target protein. The success of such an approach may depend on structural and energetic features of the particular sequestered water. Where a water molecule is strongly bound to the uncomplexed protein, it may be advantageous to incorporate binding interactions directed *via* such a water molecule. Such factors may have contributed to the poorer affinity generated on replacing a bound water by a hydroxyl substituent in the cyclosporin A−cyclophilin A system (Mikol et al., 1995). Our understanding of the thermodynamic contributions of water at the binding interface, and hence the energetic and structural requirements for designed replacements, should improve as further data are accumulated.

ACKNOWLEDGMENT

We acknowledge the technical assistance of Sarah Brockbank in the construction of the strains used in cloning the mutant 24 kDa fragment of the *E. coli* gyrase B protein. We thank Professor Janet Thornton (University College, London) for her advice on histidine conformations.

REFERENCES

Ali, J. A., Jackson, A. P., Howells, A. J., & Maxwell, A. (1993) *Biochemistry 32*, 2717−2724.

Ali, J. A., Orphanides, G., & Maxwell, A. (1995) *Biochemistry 34*, 9801−9808.

Allen, F. H., & Kennard, O. (1993) *Chem. Design Automation News 8*, 31−37.

Bailey, D., Cooper, J. B., Veerapandian, B., Blundell, T. L., Atrash, B., Jones, D. M., & Szelke, M. (1993) *Biochem. J. 289*, 363−371.

Becker, J. W., Rotonda, J., McKeever, B. M., Chan, H. K., Marcy, A. I., Wiederrecht, G., Hermes, J. D., & Springer, J. P. (1993) *J. Biol. Chem. 268*, 11335−11339.
Berger, J. M., Gamblin, S. J., Harrison, S. C., & Wang, J. C. (1996) *Nature 379*, 225−232.
Bernstein, F. C., Koetzle, T. F., Williams, G. J. B., Meyer, E. F., Jr., Brice, M. D., Rodgers, J. R., Kennard, O., Shimanouchi, T., & Tasumi, M. (1977) *J. Mol. Biol. 112*, 535−542.
Bhat, T. N., Bentley, G. A., Boulot, G., Greene, M. I., Tello, D., Dall'Acqua, W., Souchon, H., Schwarz, F. P., Mariuzza, R. A., & Poljak, R. J. (1994) *Proc. Natl. Acad. Sci. U.S.A. 91*, 1089−1093.
Blundell, T. L., Jenkins, J. A., Sewell, B. T., Pearl, L. H., Cooper, J. B., Tickle, I. J., Veerapandian, B., & Wood, S. P. (1990) *J. Mol. Biol. 211*, 919−941.
Boles, M. O., & Taylor, D. J. (1975) *Acta Crystallogr. B 31*, 1400.
Brand, J. G., & Toribara, T. Y. (1972) *Mol. Pharmacol. 8*, 751−758.
Brünger, A. T., Kuriyan, J., & Karplus, M. (1987) *Science 235*, 458−460.
Bundle, D. R., & Sigurskjold, B. W. (1995) *Methods Enzymol. 247*, 288−305.
CCP4 (1994) *Acta Crystallogr. D 50*, 760−763.
Chervenak, M. C., & Toone, E. J. (1994) *J. Am. Chem. Soc. 116*, 10533−10539.
Connelly, P. R., Thomson, J. A., Fitzgibbon, M. J., & Bruzzese, F. J. (1993) *Biochemistry 32*, 5583−5590.
Contreras, A., & Maxwell, A. (1992) *Mol. Microbiol. 6*, 1617−1624.
Dunitz, J. D. (1995) *Chem. Biol. 2*, 709−712.
Fersht, A. R., Jackson, S. E., & Serrano, L. (1993) *Philos. Trans. R. Soc. London, Ser. A 345*, 141−151.
Freire, E. (1994) *Methods Enzymol. 240*, 502−530.
Frisch, C., Schreiber, G., Johnson, C. M., & Fersht, A. R. (1997) *J. Mol. Biol. 267*, 696−706.
Gilbert, E. J., & Maxwell, A. (1994) *Mol. Microbiol. 12*, 365−373.
Gomez, J., & Freire, E. (1995) *J. Mol. Biol. 252*, 337−350.
Gormley, N. A., Orphanides, G., Meyer, A., Cullis, P. M., & Maxwell, A. (1996) *Biochemistry 35*, 5083−5092.
Grunwald, E., & Steel, C. (1995) *J. Am. Chem. Soc. 117*, 5687−5692.
Guinto, E. R., & Di Cera, E. (1996) *Biochemistry 35*, 8800−8804.
Haberman, S. M., & Murphy, K. P. (1996) *Protein Sci. 5*, 1229−1239.
Hallet, P., Grimshaw, A. J., Wigley, D. B., & Maxwell, A. (1990) *Gene 93*, 139−142.
Hilser, V. J., Gomez, J., & Freire, E. (1996) *Proteins: Struct., Funct., Genet. 26*, 123−133.
Hu, D. D., & Eftink, M. R. (1994) *Biophys. Chem. 49*, 233−239.
Jones, T. A., Cowan, S., Zou, J.-Y., & Kyeldgaard, M. (1991) *Acta Crystallogr. A 47*, 110−119.
Ladbury, J. E., & Chowdhry, B. Z. (1996) *Chem. Biol. 3*, 791−801.
Ladbury, J. E., Wright, J. G., Sturtevant, J. M., & Sigler, P. B. (1994) *J. Mol. Biol. 238*, 669−681.
Lam, P. Y. S., Jadhav, P. K., Evermann, C. J., Hodge, C. N., Ru, Y., Bacheler, L. T., Meek, J. L., Otto, M. J., Rayner, M. L., Wong, N. Y., Chang, C. H., Weber, P. C., Jackson, D. A., Sharpe, T. R., & Erickson-Viitanen, S. (1994) *Science 263*, 380−383.
Laskowski, R. A., MacArthur, M. W., Moss, D. S., & Thornton, J. M. (1993) *J. Appl. Crystallogr. 26*, 283−291.
Lawson, C. L., Zhang, R.-G., Schevitz, R. W., Otinowski, Z., Joachimak, A., & Sigler, P. B. (1988) *Proteins: Struct., Funct., Genet. 3*, 18−31.
Lee, B., & Richards, F. M. (1971) *J. Mol. Biol. 55*, 379−400.
Lewis, R. J., Singh, O. M. P., Smith, C. V., Skarzynski, T., Maxwell, A., Wonacott, A. J., & Wigley, D. B. (1996a) *EMBO J. 15*, 1412−1420.
Lewis, R. J., Tsai, F. T. F., & Wigley, D. B. (1996b) *BioEssays 18*, 661−671.
Lisgarten, J. N., Gupta, V., Maes, D., Wyns, L., Zegers, I., Palmer, R. A., Delawis, C. G., Aguilar, C. F., & Hemmings, A. M. (1993) *Acta Crystallogr. D 49*, 541−547.
Liu, Y., & Sturtevant, J. M. (1995) *Protein Sci. 4*, 2559−2561.
Mannervik, B. (1982) *Methods Enzymol. 87*, 370−390.
Maxwell, A. (1992) *J. Antimicrob. Chemother. 30*, 409−416.
Maxwell, A. (1993) *Mol. Microbiol. 9*, 681−686.
Mikol, V., Papageorgiou, C., & Borer, X. (1995) *J. Med. Chem. 38*, 3361−3367.
Morton, C. J., & Ladbury, J. E. (1996) *Protein Sci. 5*, 2115−2118.
Naismith, J. H., Emmerich, C., Habash, J., Harrop, S. J., Helliwell, J. R., Hunter, W. N., Raftery, J., Kalb(Gilboa), A. J., & Yariv, J. (1994) *Acta Crystallogr. D 50*, 847−858.
Pauptit, R. A., Weston, S. A., Breeze, A. L., Derbyshire, D. J., Tucker, A. D., Hales, N., Hollinshead, D., & Timms, D. (1997) in *Experimental and Computational Approaches to Structure-Based Drug Design* (Codding, P. W., Ed.) Kluwer Academic Publishers, Dordrecht, The Netherlands, (in press).
Pearlman, R. S. (1982) *QCPE. 413.*
Reece, R. J., & Maxwell, A. (1991) *Nucleic Acids Res. 19*, 1399−1405.
Schwarz, F. P., Tello, D., Goldbaum, F. A., Mariuzza, R. A., & Poljak, R. J. (1995) *Eur. J. Biochem. 228*, 388−394.
Spolar, R. S., Ha, J.-H., & Record, M. T., Jr. (1989) *Proc. Natl. Acad. Sci. U.S.A. 86*, 8382−8385.
Sturtevant, J. M. (1977) *Proc. Natl. Acad. Sci. U.S.A. 74*, 2236−2240.
Sugino, A., Higgins, N. P., Brown, P. O., Peebles, C. L., & Cozzarelli, N. R. (1978) *Proc. Natl. Acad. Sci. U.S.A. 75*, 4838−4842.
Tronrud, D. E., Ten Eyck, L. F., & Matthews, B. W. (1987) *Acta Crystallogr. A 43*, 489−501.
Tsai, F. T. F., Singh, O. M. P., Skarzynski, T., Wonacott, A. J., Weston, S., Tucker, A., Pauptit, R. A., Breeze, A. L., Poyser, J. P., O'Brien, R., Ladbury, J. E., & Wigley, D. B. (1997) *Proteins: Struct., Funct., Genet. 28*, 41−52.
Van Duyne, G. D., Standaert, R. F., Schreiber, S. L., & Clardy, J. (1991) *J. Am. Chem. Soc. 113*, 7433−7434.
Vijayalakshmi, J., Padmanabhan, K. P., Mann, K. G., & Tulinsky, A. (1994) *Protein Sci. 3*, 2254−2271.
Wigley, D. B. (1996) *Structure 4*, 117−120.
Wigley, D. B., Davies, G. J., Dodson, E. J., Maxwell, A., & Dodson, G. (1991) *Nature 351*, 624−629.
Wiseman, T., Williston, S., Brandts, J. F., & Lin, L. N. (1989) *Anal. Biochem. 179*, 131−137.

BI970294+